Sub-Antenna Sparse Processing for Coherence Loss in Underwater Source Localization

Riwal LEFORT and Angélique DRÉMEAU
ENSTA Bretagne
Lab-STICC (UMR 6285)
Passive Acoustic Team
Email: riwal.lefort@ensta-bretagne.fr

***Abstract*—In underwater acoustics, inversion techniques, also called "Matched Field" processing, remain the best methods for locating acoustic sources. But this is without counting on the environmental parameter fluctuations that lead to injurious coherence loss.**

We have shown in a previous work that a sub-antenna approach could be well suited to deal with such coherence loss, however at the expense of a lower resolution. In this paper, we propose to solve this drawback by considering sparse priors.

In the experimental part of this paper, by using numerical simulations of plane waves subject to coherence loss, we demonstrate that the proposed method not only outperforms a classical beamformer in terms of source localization performance, but also, that it improves the antenna resolution.

I. Introduction

In underwater acoustics, the Conventional Beamforming (CB) [1] is the most popular method for assessing a source position. In order to improve its power resolution, so-called "high-resolution" techniques have then been proposed, distinguishing by the a priori information they consider on the nature and/or the number of sources. Among them, we can mention the well-known Minimum Variance Distortionless Response (MVDR) beamformer [2], the MUltiple SIgnal Classification (MUSIC) beamformer [3] and, more recently, sparse techniques [4].

In this latter context, the most common methods probably remain the greedy algorithms, including Orthogonal Matching Pursuit (OMP) [5] or Simultaneous OMP (SOMP) [6] when considering multiple measurements . In underwater acoustics, we can also mention the use of convex-relaxation based algorithms, such as the Least Absolute Shrinkage and Selection Operator (LASSO) [4] or the Simultaneous LASSO (SLASSO) when considering multiple measurements (snapshots) [7]. All these latter techniques offer a high resolution, but are intrinsically not designed to be robust to random environmental fluctuations such as internal waves or sound speed spatio-temporal dynamics. These fluctuations lead in practice to a not predictable coherence loss of the measured pressured field. Consequently, mislead by a wrong physical model, inversion techniques fail in recovering the source positions.

Flatté *et. al.* demonstrate in [8] that the coherence loss can be interpreted as a multiplicative noise taking into account the statistical correlations between the antenna sensors. Following this assumption, we propose here a method that adapts the sparse techniques to fluctuating environments.

Formally, the paper investigates a combination of a sub-antenna approach [9], [10] with sparse techniques [4], [7]. On the one hand, sub-antenna techniques are well suited to deal with coherence loss, but at the expense of a resolution loss. On the other hand, sparse techniques alone are not designed to deal with loss of coherence, but lead to higher resolution than a simple beamformer approach. From the combination of these two approaches, we expect an improvement of both the source localization performance and the power resolution.

In this paper, we consider monochromatic sources emitting the same continuous signal. A discrete Fourier transform is used to represent the received signal at the considered frequency. Then, from an underwater antenna array measuring a complex value at each antenna sensor, we try to assess the Direction Of Arrival (DOA) of the source signals.

As a proof of concept, we propose in section V numerical simulations of far-field sources (leading to plane waves at the receiving antenna). This restriction is without loss of generality of the proposed approach. The methods, called Sub-Antenna OMP (SA-OMP) and Sub-Antenna SOMP (SA-SOMP), are compared with CB, an OMP-based beamformer and a SOMP-based beamformer.

In the two next sections II and III, we will respectively present the sparse techniques considered in this paper in the context of coherent noise and their extension to coherence loss.

II. Sparse processing for coherent model

Let $\mathbf{Y} \in \mathbb{C}^{M \times T}$ be the captured signals, where M denotes the number of sensors in the array and T denotes the number of snapshots. The signal $\mathbf{Y}$ can be expressed as a linear combination of atoms:

$$\mathbf{Y} = \mathbf{A}\mathbf{X} + \mathbf{B}, \tag{1}$$

where $\mathbf{A} \in \mathbb{C}^{M \times P}$ denotes a set of P elementary signals also called "replica" in the field of inversion, $\mathbf{X} \in \mathbb{C}^{P \times T}$

ISBN 978-0-9928626-7-1

stands for the source signal and $\mathbf{B} \in \mathbb{C}^{M\times T}$ a random white noise. We aim at finding the source signal $\mathbf{X}$.

Setting $\mathbf{Y} = [\mathbf{y}_1, \ldots, \mathbf{y}_T]$ and $\mathbf{X} = [\mathbf{x}_1, \ldots, \mathbf{x}_T]$, an immediate application of Orthogonal Matching Pursuit (OMP) is formulated as follows:

$$\begin{array}{l} \forall t \in \{1, \ldots, T\}, \\ \tilde{\mathbf{x}}_t = \arg\min\limits_{\mathbf{x}_t} \|\mathbf{y}_t - \mathbf{A}\mathbf{x}_t\|_2^2, \\ \text{s.t. } \mathbf{x}_t \text{ has at most } L \text{ nonzero components,} \end{array} \tag{2}$$

where $\|.\|_2$ denotes the the ℓ_2-norm.

The results of the T optimization processes can then be combined by averaging their contributions, leading to the OMP beamformer power spectrum $\mathbf{P}_{\text{OMP}} \in \mathbb{R}^P$ whose ith element $\mathbf{P}_{\text{OMP}}(i)$ is such as

$$\mathbf{P}_{\text{OMP}}(i) = ||\tilde{\mathbf{X}}(i)||_2^2, \tag{3}$$

where $\tilde{\mathbf{X}}(i)$ is the ith row of matrix $\tilde{\mathbf{X}} \triangleq [\tilde{\mathbf{x}}_1, \ldots, \tilde{\mathbf{x}}_T]$.

Also exploiting a sparse prior on the sources, Simultaneous OMP (SOMP) distinguishes from OMP by taking into account an additional information over the signal to recover, more particularly by explicitly formalizing its stationarity. In practice, SOMP considers the Frobenius matrix norm $\|.\|_F$ of the matrix $\mathbf{X}$ instead of the ℓ_2-norm of each column $\mathbf{x_t}$. The optimization problem takes then the following form

$$\begin{array}{l} \tilde{\mathbf{X}} = \arg\min\limits_{\mathbf{X}} \|\mathbf{Y} - \mathbf{A}\mathbf{X}\|_F^2, \\ \text{s.t. } \mathbf{X} \text{ has at most } L \text{ nonzero rows.} \end{array} \tag{4}$$

The SOMP beamformer power spectrum $\mathbf{P}_{\text{SOMP}}$ is obtained by considering the same pooling strategy as in equation (3).

III. Sparse processing for coherent loss

A. Non coherent model

Formally, model (1) does not take into account any coherence loss. The replicas are assumed to be perfectly known, without any random perturbation due to environmental fluctuations. As suggested in [8], the spatio-temporal dynamics of the environment can take the form of a multiplicative noise $\mathbf{\Phi} \in \mathbb{C}^M$ perturbing the "coherent" acoustic field. Adopting such a model, the measured acoustic field is then formalized as follows

$$\mathbf{Y} = \text{diag}(\mathbf{\Phi})\mathbf{A}\mathbf{X} + \mathbf{B}, \tag{5}$$

where $\text{diag}(\mathbf{\Phi})$ is the diagonal matrix whose diagonal is $\mathbf{\Phi}$.

B. Coherent sub-antenna model

Assuming an unknown $\mathbf{\Phi}$ leads to a much more difficult DOA estimation problem since it introduces randomness on the observation model. To solve this problem, we propose here to proceed by sub-space projections.

Let $\mathbf{W}_k \in \mathbb{R}^{M\times M}$ be a projection matrix that actually designs the shape of a sub-antenna. For a Gaussian shape, the mth diagonal element of the matrix $\mathbf{W}_k$ is given by

$$\exp\left(\frac{-(k-m)^2}{2\gamma^2}\right), \quad \forall m \in \{1, \ldots, M\}, \tag{6}$$

the other elements being set to 0. For a rectangular shape, the one we propose to use in this paper, it is expressed by

$$\begin{cases} 1, \text{ if } |k-m| < \gamma \\ 0, \text{ if } |k-m| > \gamma. \end{cases} \tag{7}$$

In both expressions (6) and (7), the parameter $\gamma \in \mathbb{R}^+$ approximates the average coherence length C_L which is the maximum distance where two sensors remain statistically correlated.

Multiplying both sides of equation (5) by the projection matrix, we get the sub-antenna model

$$\mathbf{W}_k\mathbf{Y} = \mathbf{W}_k\text{diag}(\mathbf{\Phi})\mathbf{A}\mathbf{X} + \mathbf{W}_k\mathbf{B}. \tag{8}$$

The underlying idea behind such an operation is the assumption that on each sub-antenna, there is not any loss of coherence. In other words, we suppose here that each sensor in the antenna is locally correlated with its neighboring sensors. Formally, this is equivalent to say that the coherence loss has a constant value on a sub antenna. Let $\phi_k \in \mathbb{C}$ be this value and $\mathbf{X}_k \triangleq \phi_k\mathbf{X}$. The model (8) can then be simplified into the form of

$$\mathbf{W}_k\mathbf{Y} = \mathbf{W}_k\mathbf{A}\mathbf{X}_k + \mathbf{W}_k\mathbf{B}. \tag{9}$$

This sub-antenna trick allows us to convert the non-coherent model (5) into the form of the coherent model (1). We propose now to find a sparse solution in each of the sub-antennas.

C. Sparse sub-antenna pooling

In this paper, and contrary to the approach proposed in [9], we resort to as many sub-antennas as the number of sensors in the entire antenna. Therefore, we handle a set of M projection matrices: $\{\mathbf{W}_1, \ldots, \mathbf{W}_M\}$, defined as in equations (6) or (7).

For each coherent model (9), we can then find a sparse solution $\tilde{\mathbf{X}}_k \triangleq [\tilde{\mathbf{x}}_{k,1}, \ldots, \tilde{\mathbf{x}}_{k,T}]$ by using the OMP approach:

$$\begin{array}{l} \tilde{\mathbf{x}}_{k,t} = \arg\min\limits_{\mathbf{x}_{k,t}} \|\mathbf{W}_k\mathbf{y}_t - \mathbf{W}_k\mathbf{A}\mathbf{x}_{k,t}\|_2^2, \forall k, \forall t, \\ \text{s.t. } \mathbf{x}_{k,t} \text{ has at most } L \text{ nonzero components,} \end{array} \tag{10}$$

or, equivalently, the SOMP approach:

$$\begin{array}{l} \tilde{\mathbf{X}}_k = \arg\min\limits_{\mathbf{X}_k} \|\mathbf{W}_k\mathbf{Y} - \mathbf{W}_k\mathbf{A}\mathbf{X}_k\|_F^2, \forall k \\ \text{s.t. } \mathbf{X}_k \text{ has at most } L \text{ nonzero rows.} \end{array} \tag{11}$$

The resulting sub-antenna power spectrum, say $\mathbf{P}_{\text{SA}}$, can be obtained by a similar pooling strategy to the one proposed in (3), extended to the sub-antenna context as follows

$$\mathbf{P}_{\text{SA}}(i) = \frac{\sum_{k=1}^M ||\tilde{\mathbf{X}}_k(i)||_2^2}{\sum_{k=1}^M ||\tilde{\mathbf{X}}_k(i)||_0}, \tag{12}$$

where $||\tilde{\mathbf{X}}_k(i)||_0$ counts the number of non-zero elements in the ith row of $\tilde{\mathbf{X}}_k$.

A summary of each step of the proposed approach is given in **Algorithm 1**.

ISBN 978-0-9928626-7-1 © EURASIP 2017

Algorithm 1 Sub-antenna sparse pooling (SA-OMP or SA-SOMP)

1: **for** $k = 1$ to M **do**
2: Compute $\mathbf{W}_k$ by using (6) or (7)
3: Compute $\tilde{\mathbf{X}}_k$ by using (10) or (11)
4: **end for**
5: Compute the beamformer output $\mathbf{P}_{\text{SA}}$ by using (12)

D. Discussion

Using sparse techniques like OMP and SOMP usually requires to know the exact number of sources, say N, the number of nonzero components being thus set to $L = N$. In this paper, for both SA-OMP and SA-SOMP, the number of nonzero components L rather controls the beamformer power spreading that is the outcome of the pooling process (12). As illustrated in Figure 2, this process allows us to concentrate the maximum power around the source directions and thus improve the resolution. Note that this is not equivalent to increase the value of L in the case of OMP and SOMP. Doing so would produce a power spectrum in the form of a comb but more likely to be mistaken in the case of environmental fluctuations. In this paper, the number of nonzero components L is therefore considered as a free parameter that is not necessarily correlated with the number of sources N. For instance, Figure 3 is obtained by setting $L = 2$ although $N \in \{1, \ldots, 6\}$. To conclude this remark, we need to stress that, unlike OMP and SOMP, both methods SA-OMP and SA-SOMP can be used without knowing the number of sources.

IV. Numerical simulation of coherence loss

In [8], it is shown that the loss of coherence can be represented by a multiplicative noise. Following this idea, we simulate the loss of coherence by simulating a multiplicative noise $\mathbf{\Phi}$ obeying a Gaussian law. We make the additional assumption that the random process $\mathbf{\Phi}$ is stationary, or in other words, the fluctuations are assumed to be stable in time. We then have

$$\mathrm{p}(\mathbf{\Phi}) = \mathcal{CN}\left(\mathbf{0}, \mathbf{\Sigma}\right), \tag{13}$$

where $\mathcal{CN}$ stands for a circular complex Gaussian law. The covariance matrix $\mathbf{\Sigma}$ allows us to control the targeted coherence length C_L which is the maximum distance where two sensors remain statistically correlated. Formally, the expression of the (m_1, m_2)th component of the covariance matrix $\mathbf{\Sigma}$ is given $\forall (m_1, m_2) \in \{1, \ldots, M\}^2$, by

$$\mathbf{\Sigma}(m_1, m_2) = \exp\left(\frac{-(m_1 - m_2)^2}{2C_L^2}\right). \tag{14}$$

In Figure 1 we show some random realizations of the coherent loss $\mathbf{\Phi}$ such as $C_L \in \{1, 10, 20, 40\}$. The phase of $\mathbf{\Phi}$ is reported as a function of the sensor index. As expected, we observe that the less the coherence length C_L the more the noise perturbation.

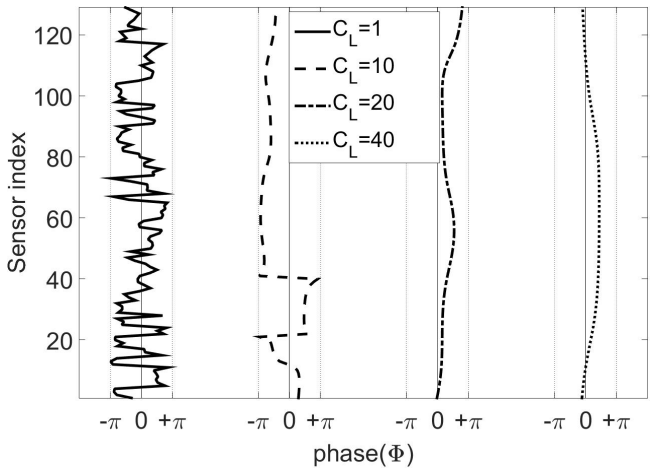

Fig. 1. Some random realizations of the multiplicative noise Φ. The phase of Φ is reported as a function of the sensor index for different coherent length $C_L \in \{1, 10, 20, 40\}$. In this experiment the number of sensors is set to $M = 128$.

V. Experiments

In this section, we propose extensive synthetic experiments to assess the performance of the proposed approach. In these experiments, we consider the numerical simulation of plane waves that are captured by a linear array composed of $M = 128$ sensors. The sensors are uniformly distributed such that the distance between two consecutive sensors is set to $\Delta = 0.4\,\lambda$ meters, where $\lambda = c/f$ denotes the wave length in meters, $c = 1500$ meter/second denotes the sound speed and $f = 1000$ Hz denotes the signal frequency. The analytic expression of each atom $\mathbf{A}(i) \in \mathbb{C}^{M \times 1}$, such as $\mathbf{A} = [\mathbf{A}(1), \ldots, \mathbf{A}(P)]$, is given by

$$\mathbf{A}(i) = \left\{ e^{j\frac{2\pi}{\lambda}(m-1)\Delta \sin(\theta(i))} \right\}_{m \in \{1,\ldots,M\}}, \tag{15}$$

where $\theta(i)$ denotes the Direction-Of-Arrival (DOA) of the acoustic signal in radian regarding the antenna position.

In the two following subsections, we respectively conduct a qualitative and quantitative analysis to characterize the antenna resolutions and evaluate the capacity of a beamformer to localize each source.

A. Subjective analysis of the power resolution

In Figure 2 we present a subjective analysis of the resulting antenna resolution. Each beamformer power spectrum is displayed as a function of the direction angle. Both proposed methods SA-OMP and SA-SOMP are compared with CB. In this experiment, each sub-antenna sparse solution is obtained such that $L = 2$. The sub-antennas are designed from the rectangular shape of equation (7) such that $\gamma = 6$. The random coherence loss is simulated by using the covariance matrix (14), where the coherence length is set to $C_L = 20$. In addition, we consider an additive white noise such that the Signal-to-Noise-Ratio is set to SNR=10dB. We consider either two uniformly

ISBN 978-0-9928626-7-1 © EURASIP 2017

distributed sources (Fig 2-a) or four uniformly distributed sources (Fig 2-b). In this experiment, we consider $T = 100$ snapshots.

As expected, around the true source position, there is no major difference between each beamformer. But, when the angle differs from the optimal solutions, the SA-OMP power and the SA-SOMP power tend to $-\infty$, while it is stuck to -35 dB for a CB. This goes in the favour of the proposed methods.

At this point, it is difficult to observe a difference between SA-OMP and SA-SOMP, even if the resolution seems to be better with SA-SOMP. The explanation is that SOMP provides the same zero components for each snapshot, contrary to OMP that may propose different zero components for each snapshots. The consequence is that OMP provides more solutions than SOMP and that OMP spreads the beamformer power and consequently decreases the power resolution.

B. Quantitative analysis by ROC curves area and Monte Carlo iterations

In the previous section we have illustrated the good behavior of the proposed approaches with regard to the resolution, in this section we perform a quantitative analysis to evaluate the beamformer capacity to localize each source. Five beamformers are compared: SA-OMP, SA-SOMP, OMP, SOMP and CB. In this experiment, the number of snapshots is set to $T = 20$. The coherence loss is modelled by using the covariance matrix (14), where the coherence length is set to $C_L = 20$. In addition, we consider an additive noise such that the SNR is set to SNR=-10 dB in Figure 3-a while it is set to SNR=10 dB in Figure 3-b.

In order to average the results, we consider 500 Monte Carlo iterations. At each iteration, the source positions are randomly sampled and we add a random phase change in $[-\pi, \pi]$. The ROC curve areas are computed to measure how much each beamformer power is ranked in the same way as the ground truth. In Figure 3, the ROC curve area, averaged through the 500 Monte Carlo iterations, is reported as a function of the number of sources. The closer to 1 the ROC curve area the better the localization performance.

In these experiments, the sub-antenna shape is rectangular, according to equation (7), such that $\gamma = C_L$, *i.e.* knowing the coherence length. In addition, the number of zero components is set to $L = 2$. For OMP and SOMP, the number of nonzero components is set to the exact number of sources: $L = N$.

Two remarks can be done at this point. Firstly, both proposed methods SA-OMP and SA-SOMP outperform the standard sparse beamformers OMP and SOMP. This result tends to show that the sub-antenna pooling process (12) allows us to improve the simple snapshot pooling method (3). Secondly, despite both a loss of coherence and a random white noise, the proposed method not only allows us to improve the antenna resolution (section V-A), but also, it outperforms, or at least gives similar results to, the conventional beamformer CB.

(a) 2 sources at $\{-0.37, 0.32\}$ radian

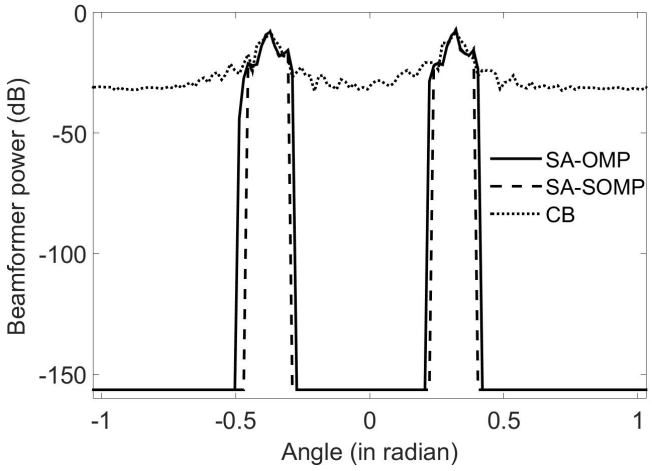

(b) 4 sources at $\{-0.65, -0.23, 0.17, 0.58\}$ radian

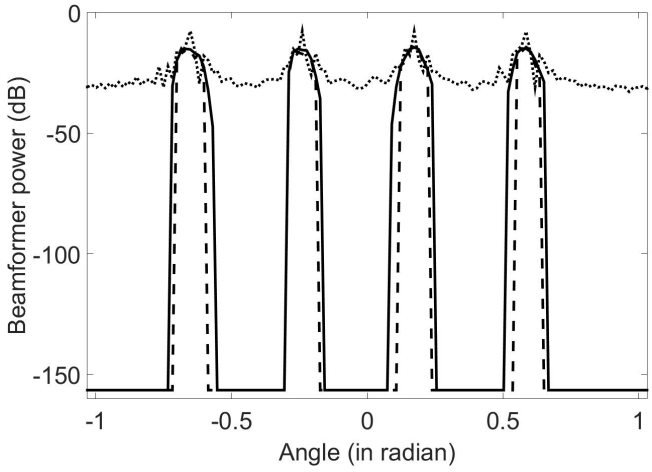

Fig. 2. In this subjective analysis, we propose to compare the beamformer powers in decibels of our Sub-Antenna Orthogonal Matching Pursuit (SA-OMP) and our Sub-Antenna Simultaneous Orthogonal Matching Pursuit (SA-SOMP) with the powers of a conventional beamformer (CB). We consider either 2 sources (Fig. 2-a) or 4 sources (Fig. 2-b). In this experiment, we consider $M = 128$ sensors, $T = 100$ snapshots, $P = 128$ atoms in the dictionary, an additive white noise such that the Signal-to-Noise-Ratio equals SNR=10 dB and a coherence length of $C_L = 20$.

We additionally observe that SA-OMP outperforms SA-SOMP in less noisy cases as illustrated in Figure 3-b. The reason is that SA-SOMP offers less variability than SA-OMP, each snapshot being considered together. In other words, we have observe that the antenna resolution is better with SA-SOMP at the expense of a slight reduction of the capacity to localize.

VI. Conclusion

In underwater acoustics, the inversion techniques for the task of source localization are sensitive to environ-

ISBN 978-0-9928626-7-1 © EURASIP 2017

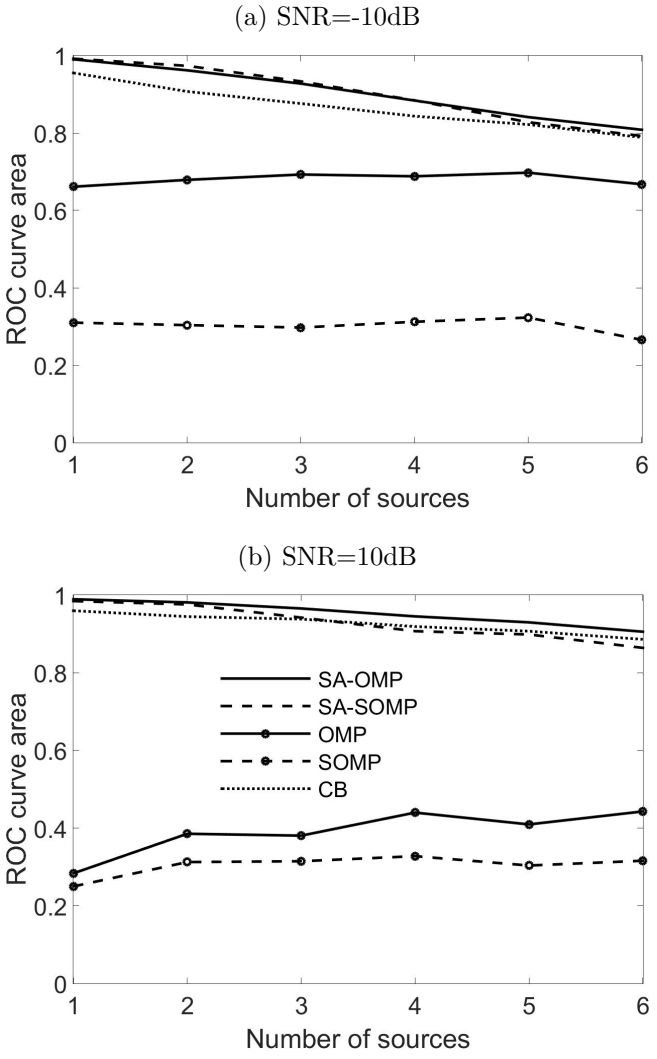

Fig. 3. In this quantitative analysis, we compare our Sub-Antenna Orthogonal Matching Pursuit (SA-OMP) and our Sub-Antenna Simultaneous Orthogonal Matching Pursuit (SA-SOMP) with the powers of a conventional beamformer (CB), an Orthogonal Matching Pursuit (OMP) and a Simultaneous Orthogonal Matching Pursuit (SOMP). For each beamformer, we report the average area under the ROC curve as a function of the number of sources. In Fig. 3-a the Signal-to-Nois-Ratio equals SNR=-10dB, while in Fig. 3-b it equals SNR=10dB. In this experiment, we consider $M = 128$ sensors, $T = 20$ snapshots, $P = 128$ atoms in the dictionary and a coherence length of $C_L = 20$. In addition, there are 500 Monte Carlo iterations to compute the average ROC curve area, some random source positions uniformly sampled at each iteration.

mental fluctuations and have to be improved accordingly. In order to deal with the resulting coherence loss, we have resorted here to sub-antenna processing, where a coherence assumption is put on each sub-antenna. Since using such an approach leads to a loss of resolution, we have proposed to combine it with sparse techniques. These methods are now well-known to perform high-resolution beamforming. Two greedy algorithms are thus considered: the popular OMP algorithm and its multiple-measurement version, the Simultaneous OMP. Both are integrated into a sub-antenna processing leading to the definition of dedicated beamforming power spectra. In the last section, we have assessed the performance of the approaches by extensive synthetic experiments simulating a far-field multi-source context. By combining both a sub-antenna processing allowing local coherence assumptions and sparse techniques compensating the resulting loss of resolution, the proposed approaches outperform standard baselines of DOA estimation.

Acknowledgment

We acknowledge funding from the DGA/MRIS.

References

[1] D.H. Johnson, D.E. Dudgeon, *Array Signal Processing: Concepts and Techniques*, Prentice Hall Signal Processing Series, pp. 1-512, 1993.

[2] J. Capon, *High-resolution frequency-wavenumber spectrum analysis*, Proceeding IEEE, vol. 57, pp. 1408-1418, 1969.

[3] G. Bienvenu, L. Kopp, *Optimality of high resolution array processing using the eigensystem approach*, IEEE Transaction on Acoustics, Speech and Signal Processing, vol. 31, no. 5, pp. 1408-1418, 1983.

[4] A. Xenaki, P. Gerstoft, K. Mosegaard, *Compressive beamforming*, Journal of Acoustical Society of America, vol. 136, no. 1, pp. 260-271, 2014.

[5] Y.C. Pati, R. Rezaiifar, P.S. Krishnaprasad, *Orthogonal matching pursuit: recursive function approximation with applications to wavelet decomposition*, Conference on Signals, Systems and Computers, 1993.

[6] J.A. Tropp, A.C. Gilbert, M.J. Strauss, *Simultaneous Sparse Approximation Via Greedy Pursuit*, International Conference on Acoustics, Speech and Signal Processing, 2005.

[7] P. Gerstoft, A. Xenaki, C.F. Mecklenbräuker, *Multiple and single snapshot compressive beamforming*, Journal of Acoustical Society of America, vol. 138, no. 4, pp. 2003-2014, 2015.

[8] S.M. Flatté, R. Dashen, W.H. Munk, K.M. Watson, F. Zachariasen, *Sound Transmission through a Fluctuating Ocean*, Part of Cambridge Monographs on Mechanics, 2010.

[9] H. Cox, *Line array performance when the signal coherence is spatially dependent*, Journal of the Acoustical Society of America, vol. 54, 1973.

[10] R. Lefort, A. Drémeau, *Spatio-temporal weighting for underwater source localization in the context of coherence loss*, Conference on Acoustic and Environmental Variability, Fluctuations and Coherence, Cambridge, UK, 2016.